20 minutes at 37°C, filtered through a 70-μm strainer, and washed in a fluorescent antibody buffer (FAB) consisting of 0.1% BSA in PBS. Supernatants from tumor tissue were collected, and homogenized cells were blocked with anti-FcR mAb for 15 minutes and followed by staining with either FITC– or PE/Cy7–anti-CD86, PE–anti-CD40, Alexa488– or peridinin-chlorophyll-protein (PerCP)–anti-CCR7, and allophycocyanin (APC)–anti-CD11c mAb either FITC–anti-CD11b, PE–anti-Gr-1, and APC–anti-F4/80, or FITC–anti-DX5, PE–anti-CD107a, and APC– or APC/Cy7–anti-CD3 mAb in FAB for 30 minutes, and subjected to multiparameter flow cytometry, a FACSCalibur or FACSVerse (BD Biosciences). Dead cells were excluded by 7-AAD staining and forward scatter/side scatter FSC/SCC profiles. Analyses of data were performed using FlowJo Version 8.8.6 software (Tree-Star). Concentrations of VEGF, TGF-β, and IL-10 in supernatants from tumor tissues were measured using Quantikine (R&D Systems) or mouse Th1/Th2 ELISA Ready-Set-Go (eBioscience).

MLR

One day after FTC, tumor-draining lymph nodes (TDLNs) and erythrocyte-depleted splenocytes were harvested from WT/WGM or KO/WGM mice as described in "Analyses for tumor-infiltrating leukocytes." DCs as stimulators (S) were purified from splenocytes or TDLNs using CD11c MicroBeads (Miltenyi Biotec). T cells as responders (R) were prepared from isolated splenocytes of C57BL/6 mice using Pan T cell isolation kit II (Miltenyi Biotec), suspended in CM supplemented with 50μM β-mercaptoethanol (Sigma-Aldrich), and cocultured with 30 Gy irradiated DCs at indicated R/T ratios on 96-well U-bottom plate for 4 days. Sixteen hours before the end of culture, 1 μCi [^{3}H]-thymidine (Moravek Biochemicals) was added to each well. Thymidine uptake was quantified in a TopCount NXT (PerkinElmer Life and Analytical Sciences). For CFSE-labeled mixed lymphocyte reaction (MLR) assay, splenic CD11c$^+$ DCs were isolated from WT/WGM or KO/WGM mice using CD11c MicroBeads (Miltenyi Biotec), irradiated with 30 Gy and cocultured with CD3$^+$ T cells as described in this section. After 6 days of coculture, the proliferation rate of CD3$^+$CD4$^+$ or CD3$^+$CD8$^+$ T cells labeled with 2.0μM CFSE (Invivogen) in the coculture was assessed by FACSVerse.

In vivo DC migration assay

Approximately 1×10^7 WGM cells were resuspended in 100 μL diluent C and incubated for 10 minutes with 1×10^{-6} M PKH26 (Sigma-Aldrich). After washing, 5×10^5 PKH26-labeled cells were subcutaneously inoculated into the right flank of WT and BLT1-KO mice. Two days after the FTC, TDLNs were homogenized by mechanical dissociation. Cell suspensions were pretreated with Fc-receptor (FcR) block and stained with FITC–anti-CD86 and APC–anti-CD11c mAb in FAB for 30 minutes. Cells were subjected to FACSCalibur or FACSVerse and analyzed using FlowJo Version 8.8.6 software.

Cytometric bead assay

Cytokine production profile from splenocytes was measured as previously described.[5] Briefly, 1 million splenocytes were harvested from WT or BLT1-KO mice challenged with WEHI3B cells or WGM cells on day 10, depleted of erythrocytes with ammonium chloride, and cocultured with or without 4×10^5 irradiated WEHI3B cells in CM for 20 hours. Production of IL-2, IL-4, IL-5, IFN-γ, and TNF-α in each supernatant was measured using Cytometric Bead Array mouse Th1/Th2 Cytokine kit (BD Biosciences), according to the manufacturer's instructions. Data were analyzed using FCAP Array Version 1.0.1 software (BD Biosciences).

Flow cytometric analysis for intracellular cytokines

On day 46 after the FTC, TDLNs or spleen were harvested from WT/WGM or KO/WGM mice (n = 3-5 per group). Homogenized cells were cultured in CM containing 50μM β-mercaptoethanol, phorbol myristate acetate (10 ng/mL), ionophore (250 mg/mL), and brefeldin A (1 ng/mL) for 4-5 hours. After washing, cells were pretreated with FcR block followed by staining with PerCP-anti–mouse CD4 mAb for 30 minutes. Subsequently, cells were fixed with 2% paraformaldehyde and stained intracellularly with FITC–anti-IFN-γ, PE–anti-IL-4, and APC–anti-IL-17A mAb in permeabilization buffer (eBioscience) for 30 minutes and subjected to FACSCalibur or FACSVerse.

Phenotypic analysis by flow cytometric analysis for diverse immune subpopulations

For mature DCs, TDLNs were harvested from the 4 groups of mice (n = 3 or 4 per group) on days 2 and 4 after the FTC. Obtained cells were blocked with FcR and stained with either FITC–anti-CD86, PE–anti-CD80, and APC–anti-CD11c mAb, or PE–anti-CD40 and APC–anti-CD11c mAb in FAB for 30 minutes. For diverse helper T subsets, TDLNs and splenocytes were harvested from WT/WGM or KO/WGM mice (n = 3-5 per group) on day 46 after the FTC. For memory T subsets, cells were stained with PE–anti-CD44, PerCP–anti-CD4, and APC–anti-CD62L mAb. For regulatory T cells, after staining with FITC–anti-CD3, PE–anti-CD25, and PerCP/Cy5.5–anti-CD4, TDLNs cells were resuspended with 100 μL Fixation/Permeabilization solution (BD Biosciences) and washed with BD Perm/Wash buffer (BD Biosciences) for 20 minutes, followed by the addition of APC–anti–FoxP3 (FJK-16; eBioscience) mAb, and incubated for 30 minutes. For other regulatory T cells, TDLNs and splenocytes were costained with FITC–anti-CD3, PE–anti-GITR, and PerCP–anti-CD4 mAb in FAB for 30 minutes, and subjected to FACSCalibur.

In vivo depletion experiments

GK1.5 and 2.43 hybridoma cells obtained from the Cell Resource Center for Biomedical Research (Institute of Development, Aging and Cancer Tohoku University) were used for the production of anti–mouse CD4 mAb and anti–mouse CD8 mAb, respectively, as previously described.[19] Briefly, these mAbs were purified with centrifugation at 53 000*g* for 20 minutes, and subjected to affinity chromatography using MAb Trap Kit (GE Healthcare). Effective depletion of CD4$^+$ and CD8$^+$ T cells was confirmed by flow cytometric analysis using splenocytes (data not shown). Mice received peritoneal injections of anti–mouse CD4 mAb, anti–mouse CD8 mAb (50 μg per mouse), or PBS for 3 days, and once every 3 days thereafter. For depletion of NK cells, mice received peritoneal injections of rabbit anti-asialo GM1 antiserum (diluted 1:20 in 200 μL PBS; Wako), on 1 day before the STC, and every 7 days thereafter.[20]

Adoptive T-cell transfer experiments

For Th17 adoptive cell transfer (ACT) therapy, Th17 cell preparation was performed as described previously[21] with minor modification. Briefly, splenic CD4$^+$ T cells from WT/WGM or KO/WGM mice on day 46 were magnetic cell sorting (MACS)-sorted using CD4$^+$T cell Isolation kit II(Miltenyi Biotec) and stimulated with plate-bound 1.0 μg/mL anti-CD3 (BD Biosciences) and 1.0 μg/mL anti-CD28 (BD Biosciences) under Th17 conditions with 1.0 ng/mL TGF-β (R&D Systems), 10 ng/mL IL-6 (R&D Systems), 5.0 μg/mL anti–IL-4 (clone 11B11), and 5.0 μg/mL anti–IFN-γ (clone XMG1.2). On day 4 after stimulation with phorbol myristate acetate and ionomycin, Th17 induction rate was confirmed to be ~ 65% among IL-17A–, IL-4–, or IFN-γ–producing T cells, and 1×10^6 cells were then intravenously injected into recipient syngeneic BALB/c mice. On the next day, they received subcutaneous challenge with 2×10^5 WEHI3B cells in the right flank. For CD4$^+$ T-cell ACT therapy, 5×10^5 splenic CD4$^+$CD44^{low} T or CD4$^+$CD44^{hi} T cells harvested from WT/WGM or KO/WGM mice were flow cytometrically (FACSAria, BD Biosciences)-sorted on day 3 after STC and injected intravenously into recipient syngeneic BLAB/c mice. They received subcutaneous challenge with 2×10^5 WEHI3B cells in the right flank.

Statistical analyses

The 2-tailed Student *t* test was used to evaluate *P* values between experimental groups. $P < .05$ was considered statistically significant.

Table 1. Comparison of the number of WGM cell-injected mice that rejected the second tumor challenge with WEHI3B cells between WT and BLT1-KO mice

	Mice that rejected first tumor challenge, no. (%)*	Mice that rejected second tumor challenge, no. (%)†
Female groups‡		
WT/WGM	30/35 (85.7)	9/30 (30.0)§
KO/WGM	16/16 (100)	13/16 (81.3)§
Male groups		
WT/WGM	0/6 (0)	—
KO/WGM	6/6 (100)	5/6 (83.3)§

— indicates not applicable.

*Assessed at day 50 after the first tumor challenge with WEHI3B or WGM cells.

†Assessed at day 50 after the second tumor challenge with WEHI3B cells.

‡Shown are combined pooled data from at least 3 independent experiments with similar results.

§χ^2 test ($P < .05$).

Survival was plotted using Kaplan-Meier curves, and statistical relevance was determined by a log-rank comparison using Prism 5 (GraphPad). All experiments were repeated at least twice.

Results

Absence of LTB4/BLT1 axis in GM-CSF–triggered immunity induces potent antitumor effects against secondary tumor challenge with WEHI3B cells

The GM-CSF production from WEHI3B cells was below detectable levels, whereas that from WGM cells was 136 ng/24 h/10^6 cells (supplemental Figure 1, available on the *Blood* Web site; see the Supplemental Materials link at the top of the online article) enough to induce substantial antitumor effects.[4,8] We compared in vitro proliferative ability between parental WEHI3B and WGM cells. Both cells exhibited an equal proliferation rate in a time-dependent manner (Figure 1A).

As myeloid cells, such as granulocytes, express abundant BLT1 and have direct antitumor effect,[22,23] we speculated that the magnitude of antitumor effect provoked by WGM cells would be attenuated when administered into BLT1-KO mice. To verify our speculation, WEHI3B cells or WGM cells (FTC) were subcutaneously inoculated into the right flank of female WT or BLT1-KO mice. WT mice challenged with WGM cells (WT/WGM mice) rejected tumor growth, whereas WT or BLT1-KO mice challenged with WEHI3B cells (WT/W or KO/W) died of tumor burden. Unexpectedly, BLT1-KO mice challenged with WGM cells (KO/WGM mice) also significantly rejected tumor growth ($P < .05$; Figure 1C). We next compared antitumor responses against secondary tumor challenge with WEHI3B cells long after the FTC rejection. On day 50 after the FTC, parental WEHI3B cells (STC) were subcutaneously inoculated into the opposite (left) flank of WT/WGM and KO/WGM mice that had completely rejected the FTC. Intriguingly, KO/WGM mice significantly again rejected the outgrowth of STC ($P < .01$; Figure 1D) and survived for significantly longer periods compared with WT/WGM mice ($P < .01$; Figure 1E; Table 1). Similar results were observed in experiments using male mice, showing no sexual difference in the STC-rejection mechanism (Table 1).

Previous studies have reported that LTB4 antagonists inhibit cell proliferation of several cancer cells.[24,25] To exclude the possibility that the rejection of STC was attributable to blocking of the LTB4/BLT1 axis-mediated direct antiproliferative effects, we examined BLT1 mRNA levels in WEHI3B and WGM cells by RT-PCR analysis. Both cells expressed undetectable levels of BLT1 mRNA (supplemental Figure 2), showing that the STC rejection was not induced by inhibition of LTB4/BLT1 signaling pathway.

Absence of LTB4/BLT1 axis facilitates activation of tumor-infiltrating innate immune subpopulations with mitigated immune tolerance in GM-CSF-induced antitumor immunity

We hypothesized that the rejection of STC could be induced by memory antitumor immunity. As GM-CSF–producing tumor cell vaccines not only induce the potent antitumor immunity by enhanced maturation of DCs[26] but also simultaneously recruit abundant immune-regulatory myeloid-derived suppressor cells (MDSCs),[27] we investigated the effect of blockade of LTB4/BLT1 signaling on tumor-infiltrating GM-CSF–sensitized diverse subsets of innate immune cells in early phase. The number of MDSCs and macrophages in tumors from KO/WGM mice were significantly decreased compared with those from WT/WGM mice ($P < .05$; Figure 2A-B). In contrast, the cell numbers of tumor-infiltrating NK cells, natural killer-like T cells (NKT), and cytolytic NK cells harvested from KO/WGM mice were significantly increased compared with those from WT/WGM mice (Figure 2C-E). In addition, the defective LTB4/BLT1 axis enhanced maturation of tumor-infiltrating DCs in tumors from KO/WGM mice compared with those from WT/WGM mice, as demonstrated by significantly increased expression of DC maturation markers, such as CD40 and CCR7 ($P < .05$; Figure 2F). Similar results were obtained for $CD86^+CD40^+$DCs, $CD40^+CCR7^+$DCs, $CCR7^+CD86^+$DCs, and $CD86^+CD40^+CCR7^+$DCs isolated from tumors ($P < .05$; Figure 2G-H). We subsequently compared the expression of the immune-regulatory cytokines VEGF, TGF-β, and IL-10 at the tumor injection site that might account for various DC maturation. Concentrations of VEGF, TGF-β, and IL-10 in the supernatants derived from single-cell suspensions of excised tumors from KO/WGM mice were significantly lower than those of WT/WGM mice ($P < .05$; Figure 2I). Lastly, to examine the effect of the defective LTB4/BLT1 axis on GM-CSF–primed DCs for T-cell activation, we performed MLR assay using allogeneic T cells from C57BL/6 mice and splenic- or TDLN-derived $CD11c^+$ DCs. The results showed that both splenic- (Figure 2J left panel) and TDLN- (Figure 2J right panel) derived DCs harvested from KO/WGM mice stimulated $CD3^+$ T cells more efficiently than those from WT/WGM mice. When we compared the stimulation capacity of DCs harvested from KO/WGM mice for $CD4^+$ and $CD8^+$ T cells, we observed a superior proliferation of $CD4^+$ T cells but not $CD8^+$ T cells (Figure 2K).

Absence of LTB4/BLT1 axis augments maturation and migration capacity of phagocytosed TAAs-DCs in GM-CSF-induced antitumor immunity

We next evaluated the impact of the defective LTB4/BLT1 axis on maturation of DCs in TDLNs on day 2 or 4 after FTC. As shown in Figure 3A-C and supplemental Figure 3, the mean fluorescence intensity of each CD40, CD80, and CD86 expression on DCs in TDLNs from KO/WGM mice was significantly more increased than that from WT/WGM mice ($P < .05$). To determine the influence of the defective LTB4/BLT1 axis on the migration

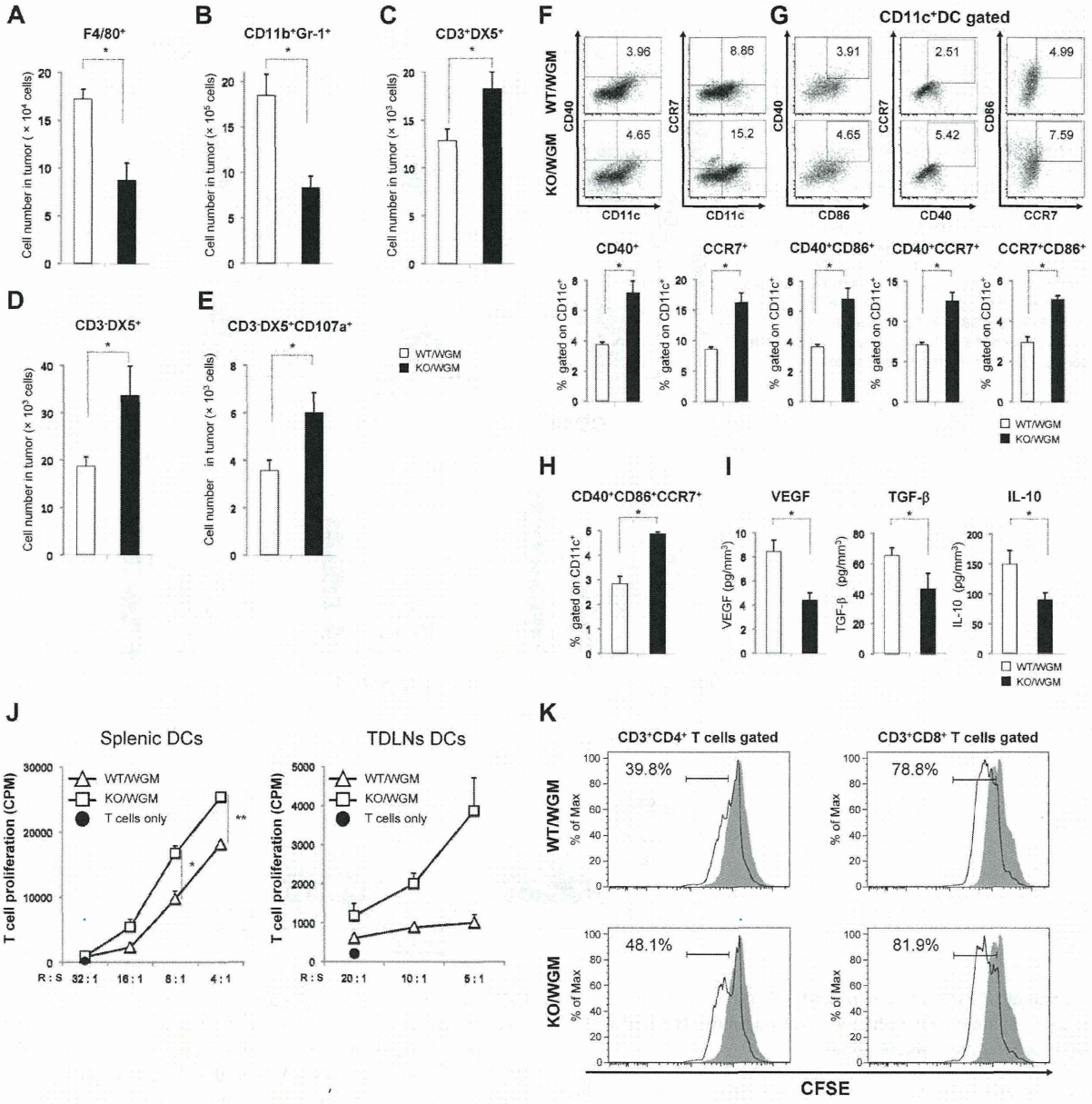

Figure 2. Absence of LTB4/BLT1 signaling promotes activation of various innate immune subpopulations in tumor tissues, accompanied with attenuated immune tolerance in KO/WGM mice. (A-E) One day after the FTC with WGM cells, tumors were excised from WT/WGM or KO/WGM mice, minced finely, and treated with collagenase for tissue dissociation. For assessment of innate immunity subpopulations, tumor infiltrating cells were subsequently analyzed by flow cytometry as described in "Analyses for tumor-infiltrating leukocytes." The numbers of viable cells are shown. (F-H) For detection of mature DCs, cells were stained with anti-CD11c, anti-CD40, anti-CD86, and anti-CCR7 mAb and subjected to flow cytometric analysis. Results shown are representative 2-dimensional dot plots (top panel, F-G) and bar graphs depicting the rates of indicated tumor infiltrating mature DCs (bottom panel, F-G). Numbers in 2-dimensional dot plots reflect the frequencies of (F) $CD40^+$ or $CCR7^+CD11c^+$cells, (G) $CD40^+CD86^+$, $CD40^+CCR7^+$, or $CCR7^+CD86^+CD11c^+$cells, and (H) $CD40^+CD86^+CCR7^+CD11c^+$ cells relative to the total $CD11c^+$ cells. (I) The concentrations of VEGF (n = 5 or 6), TGF-β (n = 3), and IL-10 (n = 9 or 10) in supernatants derived from smashed tumor tissue of WT/WGM or KO/WGM mice were measured by ELISA assay. (J) MLR assay evaluated by [^{3}H]thymidine incorporation. Various numbers of MACS-sorted splenic (left panel)- or TDLNs (right panel)-derived $CD11c^+$ DCs from WT/WGM or KO/WGM mice in early phase were 30 Gy irradiated as stimulator cells and incubated with 2×10^5 MACS-sorted splenic $CD3^+$ T cells (responder) harvested from splenic C57BL/6 mice at responder to stimulator (R:S) ratios as indicated for 4 days in triplicate. [^{3}H]Thymidine was added 16 hours before the cells were harvested, and thymidine incorporation was assessed using TopCount NXT microplate scintillation counter. Cultures in the absence of DCs (T cells only) were used as a negative control. (K) CFSE-labeled MLR assay. A total of 100 000 MACS-sorted splenic $CD11c^+$ DCs were harvested from WT/WGM or KO/WGM mice, irradiated with 30 Gy, and cocultured with $CD3^+$ T cells at an R:S ratio of 2:1. After 6 days of coculture, the proliferation rate of $CD3^+CD4^+$ T cells (left panel) or $CD3^+CD8^+$ T cells (right panel) labeled with 2.0 μM CFSE in the coculture was assessed by flow cytometric analysis. The histograms are gated on $CD3^+CD4^+$ or $CD3^+CD8^+$ T cells. Cultures in the absence of DCs (T cells only) were used as a negative control. Bar graphs represent mean ± SEM. *Significant difference ($P < .05$). **Significant difference ($P < .01$). Representative data from 3 independent experiments or combined data from 2 independent experiments (D-E) with similar results are shown.

capacity of mature DCs that had engulfed TAAs into TDLNs, we compared a proportion of $CD86^+PKH26^+$ DCs in TDLNs between WT/WGM and KO/WGM mice on day 2 after the FTC. The frequency of $CD86^+PKH26^+$ DCs in TDLNs harvested from KO/WGM mice was > 5-fold higher than that from WT/WGM mice (Figure 3D).

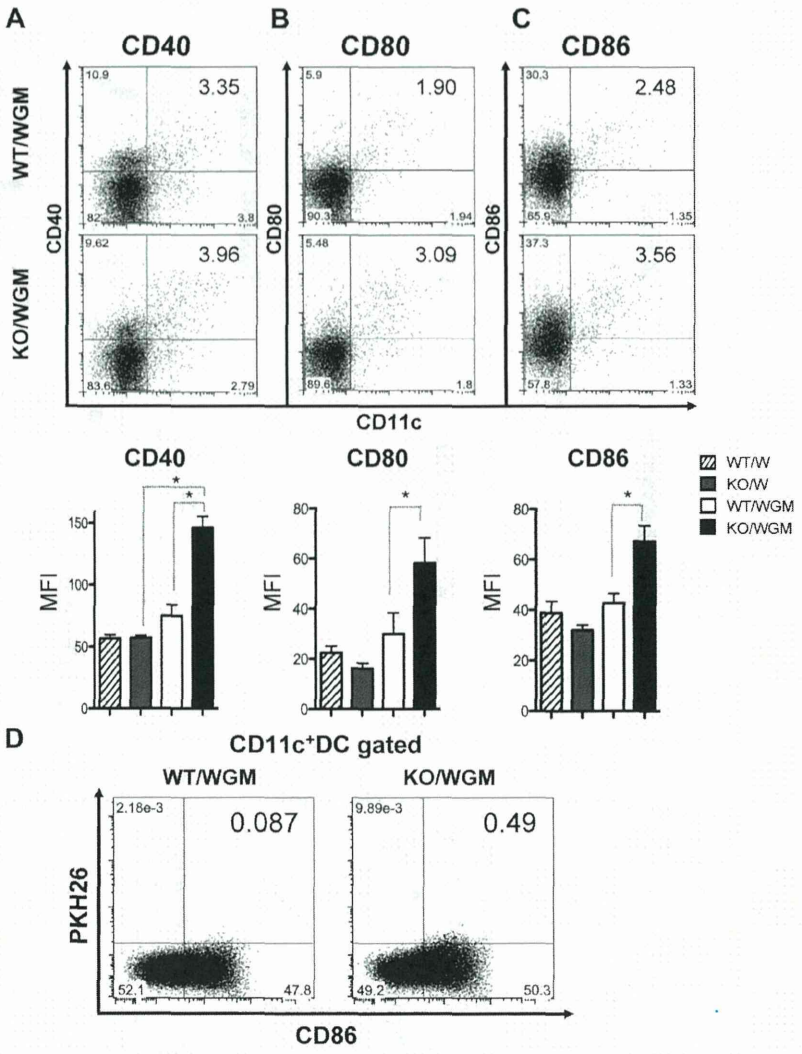

Figure 3. Absence of LTB4/BLT1 axis enhances maturation of DCs and recruitment of TAA-phagocytosed DCs into TDLNs in KO/WGM mice in early phase. Two left axillary TDLNs were harvested from WT/W, KO/W, WT/WGM, or KO/WGM mice on day 2 (CD80 and CD86) or day 4 (CD40) after the tumor challenge (n = 3-5 per group). Data are representative dot plots (top panel) and the averages of mean fluorescence intensity (bottom panel) for $CD11c^+$ cells expressing the following markers of (A) CD40, (B) CD80, or (C) CD86 in TDLNs harvested from 4 indicated experimental groups. Bar graphs represent mean ± SEM. *Significant difference ($P < .05$). (D) Migration of DCs that had phagocytosed TAAs to TDLNs in WT/WGM or KO/WGM mice on day 2 after the subcutaneous inoculation with PKH26-labeled WGM cells. *Numbers in 2-dimensional dot plots reflect the positive* ratio of $PKH26^+CD86^+$ cells relative to total $CD11c^+$ cells. Representative data from at least 3 independent experiments with similar results are shown.

Absence of LTB4/BLT1 axis in GM-CSF–induced antitumor immunity systemically enhances TAAs-specific Th1 and Th2 responses in intermediate phase

To characterize the immune-modulatory effects of the defective LTB4/BLT1 axis on GM-CSF–triggered adaptive immunity, the expression levels of inflammatory cytokines, IL-2, IFN-γ, TNF-α (Th1 cytokines), and IL-4 and IL-5 (Th2 cytokines) secreted from splenocytes harvested from KO/WGM mice were compared with those from WT/WGM mice. On the coculture with irradiated WEHI3B cells, the expression levels of IL-2, IFN-γ, TNF-α, IL-4, and IL-5 from KO/WGM mice, on day 10 after FTC, were increased compared with those from WT/WGM mice. Only levels of IL-4 were significantly altered. All other cytokines tested did not show significant differences between the 2 groups but exhibited the same tendency in 3 independent experiments (Figure 4A-E).

Absence of LTB4/BLT1 axis in GM-CSF-induced antitumor immunity increases diverse memory $CD4^+$ T subsets skewing Th balance toward Th2 and Th17 predominance with antitumor phenotype

We speculated that the defective LTB4/BLT1 axis could have a positive impact on phenotypic profile of different memory $CD4^+$ or $CD8^+$ T subset, which might account for the marked rejection of STC. Thus, we compared the rates of central memory T subset (T_{CM}) and effector memory T subset (T_{EM}) in TDLNs between WT/WGM and KO/WGM mice on day 46 in late phase. Surface marker of CD44 was used as memory phenotype. TDLNs harvested from KO/WGM mice contained significantly higher proportions of the $CD4^+CD44^+CD62L^+$ (T_{CM}) and $CD4^+CD44^+CD62L^-$ (T_{EM}) subsets relative to the total $CD4^+$ T-cell population compared with those from WT/WGM mice ($P < .05$; Figure 5A), suggesting that the defective LTB4/BLT1 axis could serve to generate long-surviving TAA-specific memory $CD4^+$ T cells. Subsequently, the proportion of Th1, Th2, and Th17 subsets in TDLNs and spleen in the late phase was evaluated between the 2 groups. The results showed that the frequency of Th2 and Th17 subset in TDLNs from KO/WGM mice increased by 32% and 47%, respectively, compared with that from WT/WGM mice (data not shown), indicating that the defective LTB4/BLT1 axis in GM-CSF–triggered immunity could cause a shift of the Th balance toward Th2 and Th17 predominance. Because IL-4 production fromTh2 cells is reported to be essential for maximal systemic antitumor immunity induced by GM-CSF–based tumor immunization,[4,28] we analyzed the total number of IL-4–producing $CD4^+$ T cells from TDLNs between the 2 groups. The total number of IL-4–producing

Th2 cells in TDLNs from KO/WGM mice was significantly higher than in WT/WGM mice ($P < .05$), suggesting that the defective LTB4/BLT1 axis facilitates effective induction of antitumor Th2 responses driven by GM-CSF (Figure 5B). To determine whether the Th17 subset has an in vivo antitumor activity, we treated recipient BALB/c mice with adoptive cell transfer of splenic Th17-skewed cells derived from WT/WGM or KO/WGM mice and subcutaneously challenged them with parental WEHI3B cells. Only the transfer of KO/WGM mice-derived Th17 cells significantly suppressed the WEHI3B tumor development compared with untreated and WT/WGM mice ($P < .05$; Figure 5C).

Furthermore, we evaluated the effect of the defective LTB4/BLT1 axis on regulatory T-cell subpopulations. The each percentage of $CD4^+CD25^+FoxP3^+$ regulatory T cells or $CD3^+CD4^+GITR^+$ cells between WT/WGM and KO/WGM mice was comparatively assessed, as GITR expression is constitutively up-regulated in regulatory T cells but not on resting $CD3^+CD4^+$ T lymphocytes.[29,30] The percentages of $CD4^+CD25^+Foxp3^+$ regulatory T cells in TDLNs and $CD3^+CD4^+GITR^+$ T cells in TDLNs and spleen from KO/WGM mice were more decreased than those from WT/WGM mice (Figure 5D-E).

Marked rejection of STC in KO/WGM mice is mainly attributed to $CD4^+$ T cells where memory Th subset possesses an antitumor phenotype

In vivo depletion of $CD4^+$ T, $CD8^+$ T, and NK cells was performed to determine which subsets are essential for the rejection of STC

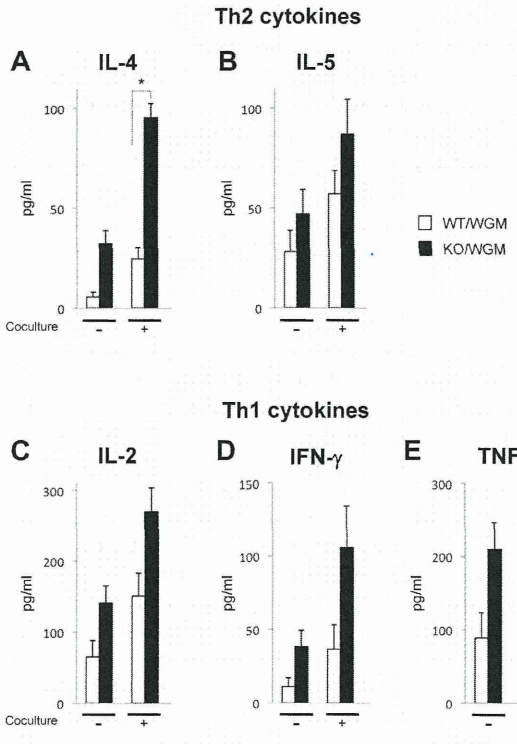

Figure 4. Absence of LTB4/BLT1 axis promotes systemic activation of TAA-specific Th1 and Th2 subsets in KO/WGM mice in intermediate phase. In vitro Th1/Th2 cytokine production profiles of splenocytes harvested from WT/W, KO/W, WT/WGM, or KO/WGM mice on day 10 after the FTC. Approximately 1×10^6 splenocytes harvested were cultured with or without 4×10^5 irradiated WEHI3B cells for 20 hours. The concentrations of mouse (A) IL-4, (B) IL-5, (C) IL-2, (D) IFN-γ, and (E) TNF-α in the culture supernatants (n = 3) were measured by cytometric bead array assay. Bar graphs represent mean ± SEM. *Significant differences ($P < .05$). Representative data from 3 independent experiments with similar results are shown.

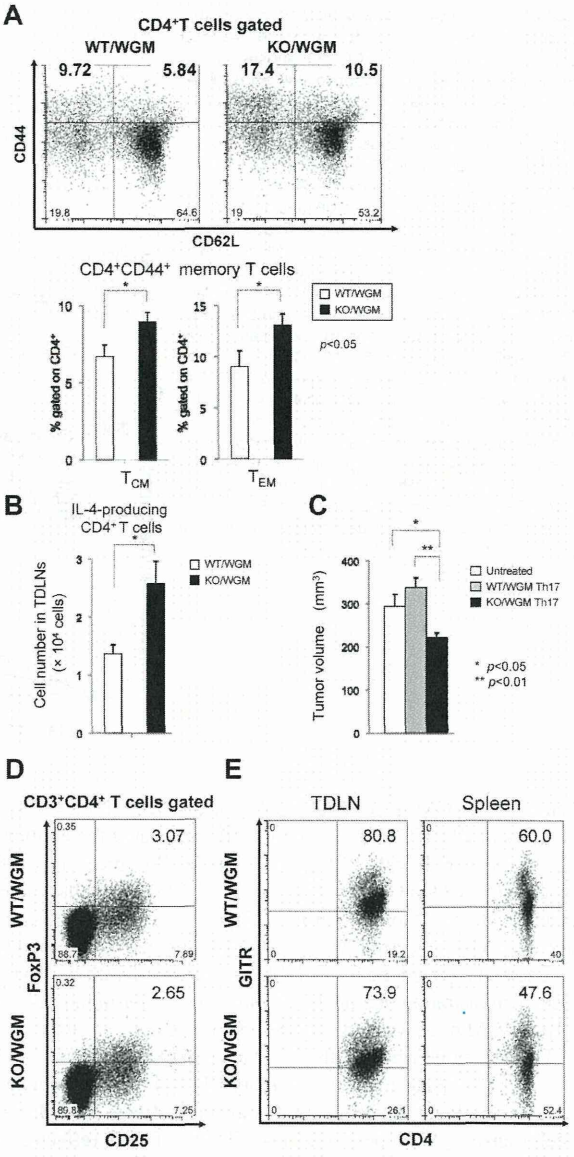

Figure 5. Absence of LTB4/BLT1 axis facilitates induction of diverse memory $CD4^+$ T subsets and polarized Th2/Th17 cells with antitumor phenotype in KO/WGM mice in late phase. TDLNs cells harvested from WT/WGM or WT/WGM mice (n = 3-5/group) on day 46 after the FTC were subjected to polychromatic flow cytometric analyses. (A) Dot plot profiles (top panels) and graphs (bottom panels) represent the percentages of $CD4^+CD44^+CD62L^+$ T_{CM} or $CD4^+CD44^+CD62L^-$ T_{EM} subset relative to the total $CD4^+$ T-cell population. Numbers in boldface in dot plot profiles show the representative percentages of T_{CM} and T_{EM} in WT/WGM and KO/WGM and are reflected to the graphs. (B) Bar graphs represent the total number of IL-4-producing T cells in TDLNs derived from WT/WGM and KO/WGM mice (n = 3 or 4). Combined data from 2 independent experiments are shown. (C) Th17 adoptive T-cell transfer (ACT) assay. Splenic $CD4^+$ T cells from WT/WGM or KO/WGM mice on day 46 were MACS-sorted and stimulated with plate-bound anti-CD3 mAb and soluble anti-CD28 mAb under Th17 condition. After 4 days of incubation, 1 million cells were intravenously transferred into recipient syngeneic BALB/c mice. On the next day, they received subcutaneous challenge with WEHI3B cells in the right flank. Bar graph represents the tumor volume (mm^3) of untreated, mice treated with WT/WGM mice- or KO/WGM mice-derived Th17 ACT, assessed on day 10 after the Th17 ACT therapy. (D-E) Phenotypic profile of immune-regulatory T cells in late phase. Shown are representative dot plots depicting the percentages of (D) $CD3^+CD4^+CD25^+FoxP3^+$ cells in TDLNs harvested from WT/WGM or KO/WGM mice, and of (E) $CD3^+CD4^+GITR^+$ T cells in TDLNs and spleen from WT/WGM or KO/WGM mice. Bar graphs represent the mean ± SEM. Significant differences: $^*P < .05$, $^{**}P < .01$. Representative data from 3 independent experiments with similar results or combined data (A-C) from 2 independent experiments are shown.

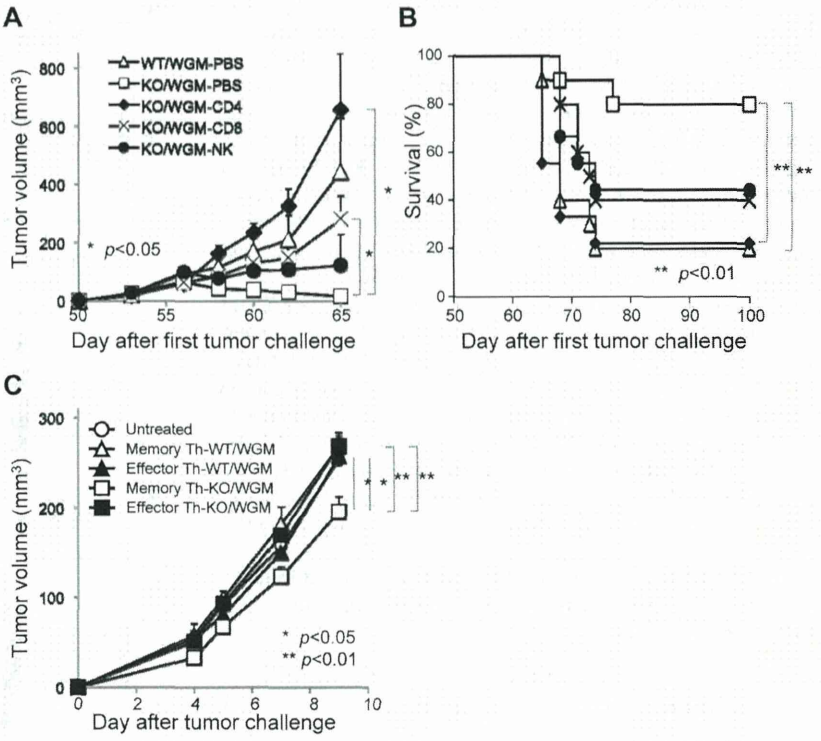

Figure 6. CD4+ T cells mainly mediate the remarkable rejection of second tumor challenge with WEHI3B cells where memory CD44hiCD4+ T subset has an antitumor phenotype on adoptive cell transfer. All mice that had completely rejected the FTC with WGM cells were then subcutaneously inoculated with the STC on day 50 after the FTC, as described in Figure 1 (n = 4-6). For depletion of CD4+ and CD8+ T cells, mice received repeated intraperitoneal injections of anti–mouse-CD4 mAb or anti–mouse-CD8 mAb on days 3, 4, and 5 before the day of the STC and once every 3 days thereafter up to 13 times. For depletion of NK cells, mice received repeated intraperitoneal injections of rabbit anti-asialo GM1 antiserum 1 day before and 7 and 14 days after the STC. (A) Tumor volume was monitored and (B) a survival curve of the mice groups was examined. (C) For CD4+ T-cell ACT therapy, 5×10^5 CD4+CD44low or CD4+CD44hi T cells harvested from spleen of WT/WGM or KO/WGM mice were flow cytometrically sorted on day 3 after the STC and intravenously injected into recipient syngeneic BLAB/c mice (n = 4-6). On the next day, they received subcutaneous challenge with 2×10^5 parental WEHI3B cells in the right flank. Bar graphs represent mean ± SEM. Significant differences: *$P < .05$, **$P < .01$. Representative or combined data from 2 independent experiments with similar results are shown.

seen in KO/WGM mice. Each depletion of CD4+ T, CD8+ T, or NK cells in KO/WGM mice significantly abrogated the antitumor effects compared with PBS-treated KO/WGM mice ($P < .05$). Importantly, KO/WGM mice depleted of CD4+ T cells elicited rather accelerated tumor outgrowth (Figure 6A) and a significantly shorter survival (Figure 6B), with a significant decrease in number of mice that rejected the STC (Table 2), compared with WT/WGM mice, demonstrating that the long-lasting antitumor immunity seen in KO/WGM mice was largely dependent on CD4+ T cells.

To determine whether the persistent antitumor memory observed in KO/WGM mice was memory CD4+ T subset-dependent, we comparatively investigated therapeutic effects by adoptive T-cell transfer (ACT) between CD4+CD44low T cells (effector Th) and CD4+CD44hi T (memory Th) cells, both of which were sorted from spleens of WT/WGM or KO/WGM mice on day 3 after the STC. We treated mice with intravenous ACT therapy and, on the next day, challenged them with WEHI3B cells in the right flank. Either with or without ACT using KO/WGM mice-derived effector Th subset, WEHI3B tumors continued to grow, whereas ACT using KO/WGM mice-derived splenic memory Th subset significantly inhibited the WEHI3B tumor formation (Figure 6C). On the other hand, all ACT therapies using cells from WT/WGM mice manifested no antitumor activity. These results strongly indicated that memory Th subset has an important role in GM-CSF–induced antitumor memory immunity when the LTB4/BLT1 signaling is not present or dysfunctional.

Table 2. Effect of in vivo depletion of each immune subpopulation on the long-lasting rejection of the second tumor challenge

Group	Mice that rejected second tumor challenge, no. (%)*
WT/WGM-PBS	1/10 (10.0)†
KO/WGM-PBS	9/11 (81.8)
KO/WGM-CD4	1/10 (10.0)†
KO/WGM-CD8	3/11 (27.3)†
KO/WGM-NK	2/10 (20.0)†

Shown are combined pooled data from 2 independent experiments with similar results.

*Assessed at day 15 after the second tumor challenge with WEHI3B cells.

†χ^2 test ($P < .05$).

Discussion

Memory T cells respond promptly to delivered antigens and are critical in the induction of sustained antitumor immunity. They require less costimulation to be activated and release a broader spectrum of cytokines compared with naive T cells.[31] One of the major challenges for therapeutic improvement of cancer vaccines is to optimize persistent memory antitumor responses.

Numerous studies reported that leukotrienes are involved in carcinogenesis and tumor development.[24,25,32,33] However, the role of leukotriene-based signaling in tumor immunology, including memory immunity, has never been elucidated. In the current study, we are the first group to find that the defective LTB4/BLT1 signaling induces long-term antitumor memory responses after immunization with WGM cells, demonstrating that the LTB4/BLT1 axis is an adversary for maintaining GM-CSF–triggered antitumor memory responses as summarized in a schematic overview (Figure 7). Namely, blockade of the LTB4/BLT1 signaling elicited numerous positive effects on development of GM-CSF–triggered persistent antitumor memory immunity as follows:

1. The defective LTB4/BLT1 axis diminished the recruitment of immune-regulatory MDSCs into tumors in early phase (Figure 2B), probably because of abundant BLT1 expression in diverse myeloid cells, including MDSCs.[34]

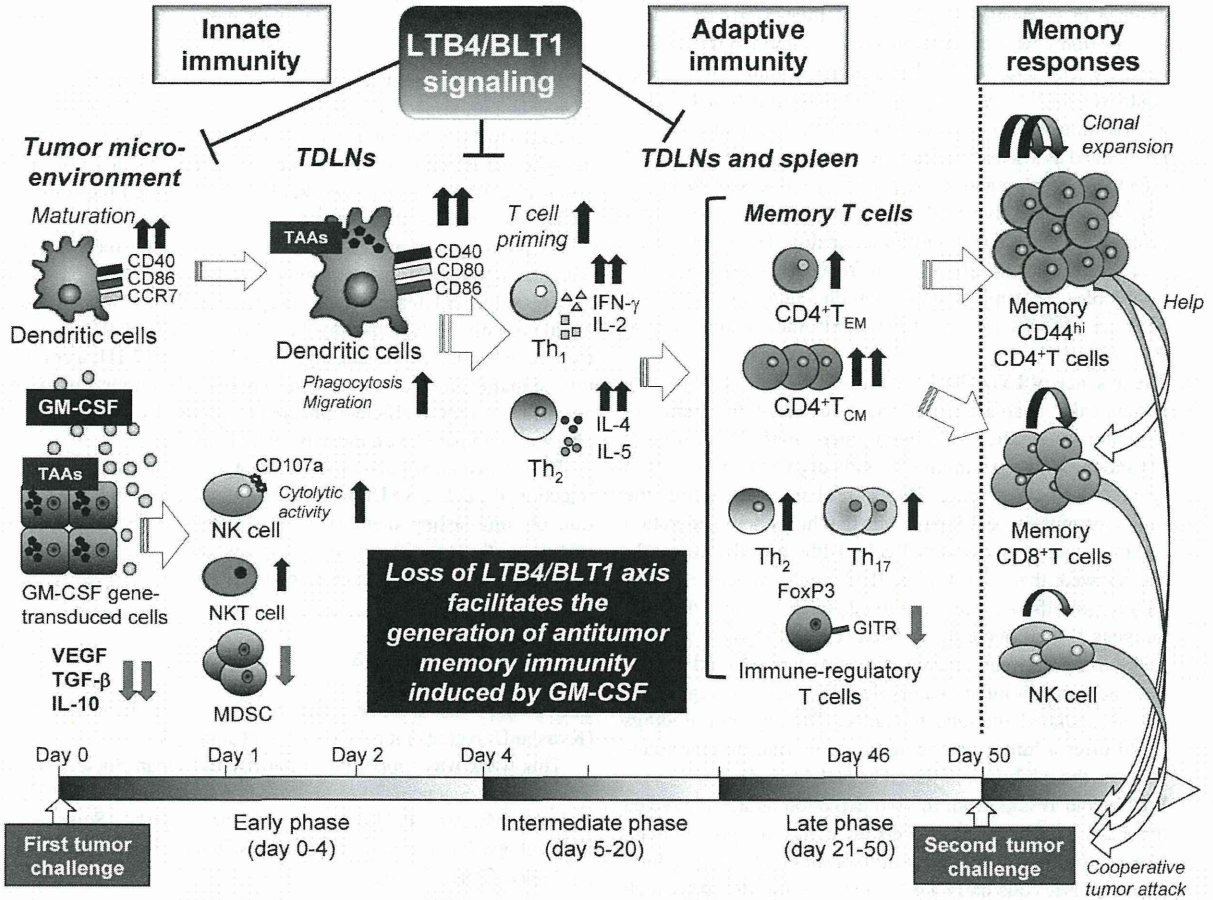

Figure 7. Schematic overview of the experimental results. This schematic overview illustrates the effects of the defective LTB4/BLT1 axis on the process of generation of antitumor memory immunity provoked by GM-CSF–transduced tumor cells in mice, and the molecular or cellular components that compose the immune system and are putatively relevant to this phenomenon.

2. The absence of LTB4/BLT1 axis increased recruitment of CD107a, a surrogate for lytic degranulation,[35] expressing cytolytic NK cells into tumors (Figure 2E), indicating its negative effects for tumoricidal ability activated by GM-CSF.
3. The defective LTB4/BLT1 signaling caused a synergistic effect on maturation, homing capacity of TAA-phagocytosed DCs into TDLNs (Figures 2F-H and 3A-D), and further enhanced the capacity of GM-CSF–sensitized DCs to stimulate $CD4^+$ T cells, but not $CD8^+$ T cells (Figure 2J-K), indicating its effective priming of helper T cell-predominant adaptive immunity. These positive effects on DCs were the result of the decreased expression of various immune-regulatory cytokines in tumor microenvironments (Figure 2I). On the contrary, others reported that LTB4 stimulation enhances DC migration and adaptive immune responses.[13] This discrepancy may stem from our use of GM-CSF gene-transduced tumor cells, although the detailed molecular crosstalk between LTB4/BLT1 and GM-CSF signaling remains unknown.
4. The absence of LTB4/BLT1 axis augmented the production of Th1 cytokine and Th2 cytokine from TAA-stimulated splenocytes harvested from GM-CSF–sensitized mice in intermediate phase (Figure 4). Conversely, Toda et al showed that functional BLT1 expression on DCs is important to initiate Th1-type immune response, indicating that GM-CSF–based immunization may bring about the conflicting outcome.[36]
5. The absence of LTB4/BLT1 axis increased the proportions of $CD4^+$ T_{CM} and $CD4^+$ T_{EM} subset in TDLNs in late phase before the STC (Figure 5A). As memory T cells possess the capacity to mount immediate recall responses to antigen challenge[37] and that T_{CM} subset has superior antitumor abilities compared with T_{EM} subset,[38] we hypothesized that the former subset might rapidly migrate to the injection site of STC to confer antitumor effects. Indeed, we succeeded to demonstrate that the KO/WGM mice-derived memory Th subset had significantly stronger antitumor efficacy than the effector Th subset from the results of ACT therapy (Figure 6C).
6. We showed that the defective LTB4/BLT1 signaling in GM-CSF-triggered antitumor immunity skewed Th2 predominance in late phase (Figure 5B) and that ACT of splenic Th17 cells harvested from KO/WGM mice elicited stronger antitumor effects against WEHI3B challenge than those from WT/WGM mice (Figure 5C). Our results are compatible with the previous reports showing that memory Th2 cells had a potent antitumor immunity through IL-4–activated NK cells[39] and that the Th17 subset was decisive for yielding immunologic responses together with effector cytotoxic T lymphocytes.[40] These findings indicate that the

absence of LTB4/BLT1 signaling facilitates Th2 and Th17 polarization with antitumor phenotype, although the significance of Th2 and Th17 cells in tumor immunology is still controversial.[41,42] As frequency of multifunctional $CD4^+$ T cells simultaneously producing IFN-γ, IL-2, and TNF-α is recognized as a sensitive immune correlate for the optimized effector function against antigens,[43] we assessed the influence of the defective LTB4/BLT1 signaling on phenotypic profiles of $CD4^+$ T-cell multifunctionality. There was, however, no significant difference in frequency of each single-, or double-, or triple-cytokine producing $CD4^+$ T subset between WT/WGM and KO/WGM mice (supplemental Figure 4).

7. The absence of LTB4/BLT1 in GM-CSF–induced immunity systemically decreased production levels of the immune-regulatory cytokines in the tumor microenvironment (Figure 2I) and the infiltrated immune-regulatory $CD4^+$ T subsets in lymphoid tissue (Figure 5D-E), probably converting the immunosuppressive milieu to one that helps both generation and maintenance of memory T cells. Although other researchers showed that LTB4 plus IL-2 could generate $CD8^+$ suppressor thymocytes involved in tolerance to self-antigens,[44] there have never been relevant data delineating relationship between arachidonic-acid–derived lipid mediator, such as pro-inflammatory leukotrienes and regulatory T cell-mediated immune tolerance. Thereby, our findings could offer a hint to attenuate tumor-driven immune tolerance via the inhibition of the LTB4/ BLT1 signaling.
8. Finally, our results from in vivo depletion assays unraveled that $CD4^+$ T cells in KO/WGM mice played a predominant role in providing persistent antitumor immunity, in coordination with NK cells and $CD8^+$ T cells (Figure 6A-B), which are compatible with the previous findings that $CD4^+$ T cells are essential in the control of tumor growth through the cooperation with macrophages and cytotoxic T lymphocytes.[4,45,46] When we consider to further clarify the molecular crosstalk between LTB4 and GM-CSF signaling pathways, it will be of importance to focus on our findings that the absence of the LTB4/BLT1 axis had positive impact mainly on $CD4^+$ helper T cell-mediated adaptive immunity as evidenced by MLR assay and ACT experiments, as well as innate immunity. This novel insight that potent memory $CD4^+$ T cells in GM-CSF–triggered immunity can be retained in devoid of LTB4/BLT1signaling allows us to expect that blocking LTB4/BLT1signaling using corresponding antagonists or inhibitors may be a promising strategy to improve the therapeutic effects of GM-CSF–based tumor vaccines in clinical settings by shaping a favorable immunologic memory.

With regard to another receptor BLT2 for LTB4, it requires very high concentrations of LTB4 for its activation[47] and has been well accepted to be a receptor for 12-HHT.[48] Accordingly, it is now thought that BLT2 does not mediate any functions of LTB4 in the absence of BLT1 in vivo. We therefore disregarded the impact of BLT2 on the results of our experiments.

Intriguingly, in terms of sexual difference, the mechanism in which a superior antitumor immunity induced by WGM cells was manifested in WT female mice compared with WT male (Table 1) could possibly be explained by the following WT regulatory T cells from female mice expressing significantly lower B7-H1, a coinhibitory signaling molecule that can suppress antitumor immunity[49] and possess a more efficient phagocytic ability by resident macrophages,[50] compared with those from male mice.

In conclusion, we demonstrated that, even long after the tumor rejection, the defective LTB4/BLT1 axis facilitates effective generation of long-lasting memory $CD4^+$ T cell-dependent antitumor immunity through its positive impacts on innate and adaptive immunologic responses induced by GM-CSF.

Acknowledgments

The authors thank Dr Kazuko Saeki and Dr Toshiaki Okuno (Kyushu University) for their technical supports.

This work was supported in part by the Japan Society for the Promotion of Science (Grant-in-Aid for Young Scientists 23790446) and the Ministry of Education, Culture, Sports, Science and Technology, Japan (Grant-in-Aid for Scientific Research on Priority Areas "Cancer" 17016053).

Authorship

Contribution: Y.Y., H.I., and K. Tani designed the study and wrote manuscript; Y.Y., H.I., Y.M., C.S., and H.N. executed the experiments; Y.Y. analyzed all data; Y.Y., H.I., T.Y., and K. Tani interpreted the results of experiments; Y.Y., H.N., A.W., and F.S. contributed in the backcross and preparation of mice; and all authors discussed the results and helped conduct experiments.

Conflict-of-interest disclosure: The authors declare no competing financial interests.

Correspondence: Kenzaburo Tani, Department of Molecular Genetics, Medical Institute of Bioregulation, Kyushu University, 3-1-1, Maidashi, Higashi-ku, Fukuoka, Japan 812-8582; e-mail: taniken@bioreg.kyushu-u.ac.jp.

References

1. Jinushi M, Tahara H. Cytokine gene-mediated immunotherapy: current status and future perspectives. *Cancer Sci.* 2009;100(8):1389-1396.
2. Tani K, Azuma M, Nakazaki Y, et al. Phase I study of autologous tumor vaccines transduced with the GM-CSF gene in four patients with stage IV renal cell cancer in Japan: clinical and immunological findings. *Mol Ther.* 2004;10(4): 799-816.
3. Dranoff G. GM-CSF-based cancer vaccines. *Immunol Rev.* 2002;188:147-154.
4. Dranoff G, Jaffee E, Lazenby A, et al. Vaccination with irradiated tumor cells engineered to secrete murine granulocyte-macrophage colony-stimulating factor stimulates potent, specific, and long-lasting anti-tumor immunity. *Proc Natl Acad Sci U S A.* 1993;90(8):3539-3543.
5. Inoue H, Iga M, Nabeta H, et al. Non-transmissible Sendai virus encoding granulocyte macrophage colony-stimulating factor is a novel and potent vector system for producing autologous tumor vaccines. *Cancer Sci.* 2008;99(11):2315-2326.
6. Salgia R, Lynch T, Skarin A, et al. Vaccination with irradiated autologous tumor cells engineered to secrete granulocyte-macrophage colony-stimulating factor augments antitumor immunity in some patients with metastatic non-small-cell lung carcinoma. *J Clin Oncol.* 2003;21(4):624-630.
7. Ho VT, Vanneman M, Kim H, et al. Biologic activity of irradiated, autologous, GM-CSF-secreting leukemia cell vaccines early after allogeneic stem cell transplantation. *Proc Natl Acad Sci U S A.* 2009;106(37):15825-15830.
8. Nakazaki Y, Hase H, Inoue H, et al. Serial analysis of gene expression in progressing and regressing mouse tumors implicates the involvement of RANTES and TARC in antitumor immune responses. *Mol Ther.* 2006;14(4):599-606.
9. Simmons AD, Li B, Gonzalez-Edick M, et al. GM-CSF-secreting cancer immunotherapies: preclinical analysis of the mechanism of action. *Cancer Immunol Immunother.* 2007;56(10):1653-1665.
10. Eager R, Nemunaitis J. GM-CSF gene-transduced tumor vaccines. *Mol Ther.* 2005;12(1):18-27.

11. Lewis RA, Austen KF, Soberman RJ. Leukotrienes and other products of the 5-lipoxygenase pathway: biochemistry and relation to pathobiology in human diseases. *N Engl J Med.* 1990; 323(10):645-655.
12. Naccache PH, Sha'afi RI. Arachidonic acid, leukotriene B4, and neutrophil activation. *Ann N Y Acad Sci.* 1983;414:125-139.
13. Del Prete A, Shao WH, Mitola S, Santoro G, Sozzani S, Haribabu B. Regulation of dendritic cell migration and adaptive immune response by leukotriene B4 receptors: a role for LTB4 in up-regulation of CCR7 expression and function. *Blood.* 2007;109(2):626-631.
14. Yokomizo T, Izumi T, Chang K, Takuwa Y, Shimizu T. A G-protein-coupled receptor for leukotriene B4 that mediates chemotaxis. *Nature.* 1997;387(6633):620-624.
15. Griffin JD, Cannistra SA, Sullivan R, Demetri GD, Ernst TJ, Kanakura Y. The biology of GM-CSF: regulation of production and interaction with its receptor. *Int J Cell Cloning.* 1990;Suppl 1:35-44.
16. Miller G, Pillarisetty VG, Shah AB, Lahrs S, Xing Z, DeMatteo RP. Endogenous granulocyte-macrophage colony-stimulating factor overexpression in vivo results in the long-term recruitment of a distinct dendritic cell population with enhanced immunostimulatory function. *J Immunol.* 2002;169(6):2875-2885.
17. Terawaki K, Yokomizo T, Nagase T, et al. Absence of leukotriene B4 receptor 1 confers resistance to airway hyperresponsiveness and Th2-type immune responses. *J Immunol.* 2005; 175(7):4217-4225.
18. Nakazaki Y, Tani K, Lin ZT, et al. Vaccine effect of granulocyte-macrophage colony-stimulating factor or CD80 gene-transduced murine hematopoietic tumor cells and their cooperative enhancement of antitumor immunity. *Gene Ther.* 1998; 5(10):1355-1362.
19. Kruisbeek AM. In vivo depletion of CD4- and CD8-specific T cells. *Curr Protoc Immunol.* 1991; Chapter 4:Unit 4 1.
20. Inoue H, Iga M, Xin M, et al. TARC and RANTES enhance antitumor immunity induced by the GM-CSF-transduced tumor vaccine in a mouse tumor model. *Cancer Immunol Immunother.* 2008;57(9): 1399-1411.
21. Nurieva R, Yang XO, Chung Y, Dong C. Cutting edge: in vitro generated Th17 cells maintain their cytokine expression program in normal but not lymphopenic hosts. *J Immunol.* 2009;182(5): 2565-2568.
22. Koga Y, Matsuzaki A, Suminoe A, Hattori H, Hara T. Neutrophil-derived TNF-related apoptosis-inducing ligand (TRAIL): a novel mechanism of antitumor effect by neutrophils. *Cancer Res.* 2004;64(3):1037-1043.
23. Di Carlo E, Forni G, Lollini P, Colombo MP, Modesti A, Musiani P. The intriguing role of polymorphonuclear neutrophils in antitumor reactions. *Blood.* 2001;97(2):339-345.
24. Tong WG, Ding XZ, Hennig R, et al. Leukotriene B4 receptor antagonist LY293111 inhibits proliferation and induces apoptosis in human pancreatic cancer cells. *Clin Cancer Res.* 2002;8(10): 3232-3242.
25. Ihara A, Wada K, Yoneda M, Fujisawa N, Takahashi H, Nakajima A. Blockade of leukotriene B4 signaling pathway induces apoptosis and suppresses cell proliferation in colon cancer. *J Pharmacol Sci.* 2007;103(1):24-32.
26. Mach N, Gillessen S, Wilson SB, Sheehan C, Mihm M, Dranoff G. Differences in dendritic cells stimulated in vivo by tumors engineered to secrete granulocyte-macrophage colony-stimulating factor or Flt3-ligand. *Cancer Res.* 2000;60(12): 3239-3246.
27. Serafini P, Carbley R, Noonan KA, Tan G, Bronte V, Borrello I. High-dose granulocyte-macrophage colony-stimulating factor-producing vaccines impair the immune response through the recruitment of myeloid suppressor cells. *Cancer Res.* 2004;64(17): 6337-6343.
28. Hung K, Hayashi R, Lafond-Walker A, Lowenstein C, Pardoll D, Levitsky H. The central role of CD4(+) T cells in the antitumor immune response. *J Exp Med.* 1998;188(12):2357-2368.
29. Shimizu J, Yamazaki S, Takahashi T, Ishida Y, Sakaguchi S. Stimulation of CD25(+)CD4(+) regulatory T cells through GITR breaks immunological self-tolerance. *Nat Immunol.* 2002;3(2): 135-142.
30. Nocentini G, Riccardi C. GITR: a multifaceted regulator of immunity belonging to the tumor necrosis factor receptor superfamily. *Eur J Immunol.* 2005;35(4):1016-1022.
31. Veiga-Fernandes H, Walter U, Bourgeois C, McLean A, Rocha B. Response of naive and memory CD8+ T cells to antigen stimulation in vivo. *Nat Immunol.* 2000;1(1):47-53.
32. Hoque A, Lippman SM, Wu TT, et al. Increased 5-lipoxygenase expression and induction of apoptosis by its inhibitors in esophageal cancer: a potential target for prevention. *Carcinogenesis.* 2005;26(4):785-791.
33. Avis IM, Jett M, Boyle T, et al. Growth control of lung cancer by interruption of 5-lipoxygenase-mediated growth factor signaling. *J Clin Invest.* 1996;97(3):806-813.
34. Yokomizo T. Leukotriene B4 receptors: novel roles in immunological regulations. *Adv Enzyme Regul.* 2011;51(1):59-64.
35. Alter G, Malenfant JM, Altfeld M. CD107a as a functional marker for the identification of natural killer cell activity. *J Immunol Methods.* 2004; 294(1):15-22.
36. Toda A, Terawaki K, Yamazaki S, Saeki K, Shimizu T, Yokomizo T. Attenuated Th1 induction by dendritic cells from mice deficient in the leukotriene B4 receptor 1. *Biochimie.* 2010;92(6):682-691.
37. Kaech SM, Wherry EJ, Ahmed R. Effector and memory T-cell differentiation: implications for vaccine development. *Nat Rev Immunol.* 2002;2(4): 251-262.
38. Fearon DT, Manders P, Wagner SD. Arrested differentiation, the self-renewing memory lymphocyte, and vaccination. *Science.* 2001;293(5528): 248-250.
39. Kitajima M, Ito T, Tumes DJ, et al. Memory type 2 helper T cells induce long-lasting antitumor immunity by activating natural killer cells. *Cancer Res.* 2011;71(14):4790-4798.
40. Kryczek I, Banerjee M, Cheng P, et al. Phenotype, distribution, generation, and functional and clinical relevance of Th17 cells in the human tumor environments. *Blood.* 2009;114(6):1141-1149.
41. Muranski P, Restifo NP. Does IL-17 promote tumor growth? *Blood.* 2009;114(2):231-232.
42. Bronte V. Th17 and cancer: friends or foes? *Blood.* 2008;112(2):214.
43. Seder RA, Darrah PA, Roederer M. T-cell quality in memory and protection: implications for vaccine design. *Nat Rev Immunol.* 2008;8(4):247-258.
44. Gualde N, Cogny van Weydevelt F, Buffiere F, Jauberteau MO, Daculsi R, Vaillier D. Influence of LTB4 on CD4−, CD8− thymocytes: evidence that LTB4 plus IL-2 generate CD8+ suppressor thymocytes involved in tolerance to self. Effect of LTB4 and IL-2 on double negative thymocytes. *Thymus.* 1991;18(2):111-128.
45. Corthay A, Skovseth DK, Lundin KU, et al. Primary antitumor immune response mediated by CD4+ T cells. *Immunity.* 2005;22(3):371-383.
46. Qin Z, Blankenstein T. CD4+ T cell–mediated tumor rejection involves inhibition of angiogenesis that is dependent on IFN gamma receptor expression by nonhematopoietic cells. *Immunity.* 2000;12(6):677-686.
47. Yokomizo T, Kato K, Terawaki K, Izumi T, Shimizu T. A second leukotriene B(4) receptor, BLT2: a new therapeutic target in inflammation and immunological disorders. *J Exp Med.* 2000;192(3):421-432.
48. Okuno T, Iizuka Y, Okazaki H, Yokomizo T, Taguchi R, Shimizu T. 12(S)-Hydroxyheptadeca-5Z, 8E, 10E-trienoic acid is a natural ligand for leukotriene B4 receptor 2. *J Exp Med.* 2008;205(4):759-766.
49. Lin PY, Sun L, Thibodeaux SR, et al. B7-H1-dependent sex-related differences in tumor immunity and immunotherapy responses. *J Immunol.* 2010;185(5):2747-2753.
50. Scotland RS, Stables MJ, Madalli S, Watson P, Gilroy DW. Sex differences in resident immune cell phenotype underlie more efficient acute inflammatory responses in female mice. *Blood.* 2011;118(22):5918-5927.

blood

2012 120: 3444-3454
doi:10.1182/blood-2011-10-383240 originally published online August 30, 2012

Absence of LTB4/BLT1 axis facilitates generation of mouse GM-CSF–induced long-lasting antitumor immunologic memory by enhancing innate and adaptive immune systems

Yosuke Yokota, Hiroyuki Inoue, Yumiko Matsumura, Haruka Nabeta, Megumi Narusawa, Ayumi Watanabe, Chika Sakamoto, Yasuki Hijikata, Mutsunori Iga-Murahashi, Koichi Takayama, Fumiyuki Sasaki, Yoichi Nakanishi, Takehiko Yokomizo and Kenzaburo Tani

Blood (print ISSN 0006-4971, online ISSN 1528-0020), is published weekly by the American Society of Hematology, 2021 L St, NW, Suite 900, Washington DC 20036.